



OPEN

Design, synthesis, and in silico studies of quinoline-based-benzo[d]imidazole bearing different acetamide derivatives as potent α -glucosidase inhibitors

Milad Noori¹, Ali Davoodi², Aida Iraj^{3,4}, Navid Dastyafteh¹, Mino Khalili¹, Mehdi Asadi², Maryam Mohammadi Khanaposhtani⁵, Somayeh Mojtavavi⁶, Mehdi Dianatpour³, Mohammad Ali Faramarzi⁶, Bagher Larijani¹, Massoud Amanlou^{2✉} & Mohammad Mahdavi^{1✉}

In this study, 18 novel quinoline-based-benzo[d]imidazole derivatives were synthesized and screened for their α -glucosidase inhibitory potential. All compounds in the series except 9q showed a significant α -glucosidase inhibition with IC_{50} values in the range of 3.2 ± 0.3 – $185.0 \pm 0.3 \mu\text{M}$, as compared to the standard drug acarbose ($IC_{50} = 750.0 \pm 5.0 \mu\text{M}$). A kinetic study indicated that compound 9d as the most potent derivative against α -glucosidase was a competitive type inhibitor. Furthermore, the molecular docking study revealed the effective binding interactions of 9d with the active site of the α -glucosidase enzyme. The results indicate that the designed compounds have the potential to be further studied as new anti-diabetic agents.

Diabetes mellitus (DM) is a chronic metabolic disease characterized by hyperglycemia, with the disorder in carbohydrate, fat, and protein metabolism in the body¹. DM is known as an important public health threat with around 450 million cases worldwide in 2019. This number is expected to rise to 700 million by 2045 worldwide confirming further action is required in this field^{2,3}. Long-term DM can increase the risk of various health complications including blindness, renal failure, foot amputation, as well as cardiovascular, retinopathy, and renal diseases⁴. Type 2 diabetes mellitus (T2DM) with around 90% of all cases is categorized as a major sub-type of DM. It was considered that glycemic control could be effective prevention and treatment for T2DM⁵⁻⁷.

α -Glucosidase (EC 3.2.1.20) is a catalytic hydrolase enzyme present on the brush border of the small intestine which hydrolyzes oligosaccharides, trisaccharides, and disaccharides to glucose and other monosaccharides at their non-reducing ends⁷⁻¹⁰. The produced monosaccharides especially glucose enter the bloodstream, resulting in postprandial hyperglycemia thus causing diabetes¹¹⁻¹³. Therefore, the inhibition of α -glucosidase might reduce carbohydrate digestion, delay glucose uptake, and consequently, decrease blood sugar levels^{14,15}. The α -glucosidase enzyme can be inhibited by acarbose, voglibose, and miglitol with sub-optimal efficacy¹⁶. Also, long-term administration of mentioned inhibitor may cause several side effects, such as abdominal pain, diarrhea, and flatulence. As a result, a need of effective inhibitors to target α -glucosidase is highly needed¹⁷⁻¹⁹.

In the last few decades, different synthetic small molecules including benzo[d]imidazole²⁰, isatin²¹ benzo[b]thiophene²² pyrimidine²³, xanthone²⁴, chromene⁶, azole^{18,25} against α -glucosidase attracted increasing attention.

¹Endocrinology and Metabolism Research Center, Endocrinology and Metabolism Clinical Sciences Institute, Tehran University of Medical Sciences, Tehran, Iran. ²Department of Medicinal Chemistry, Faculty of Pharmacy, Tehran University of Medical Sciences, Tehran, Iran. ³Stem Cells Technology Research Center, Shiraz University of Medical Sciences, Shiraz, Iran. ⁴Central Research Laboratory, Shiraz University of Medical Sciences, Shiraz, Iran. ⁵Cellular and Molecular Biology Research Center, Health Research Institute, Babol University of Medical Sciences, Babol, Iran. ⁶Department of Pharmaceutical Biotechnology, Faculty of Pharmacy and Biotechnology Research Center, Tehran University of Medical Sciences, Tehran, Iran. ✉email: amanlou@tums.ac.ir; momahdavi@tums.ac.ir

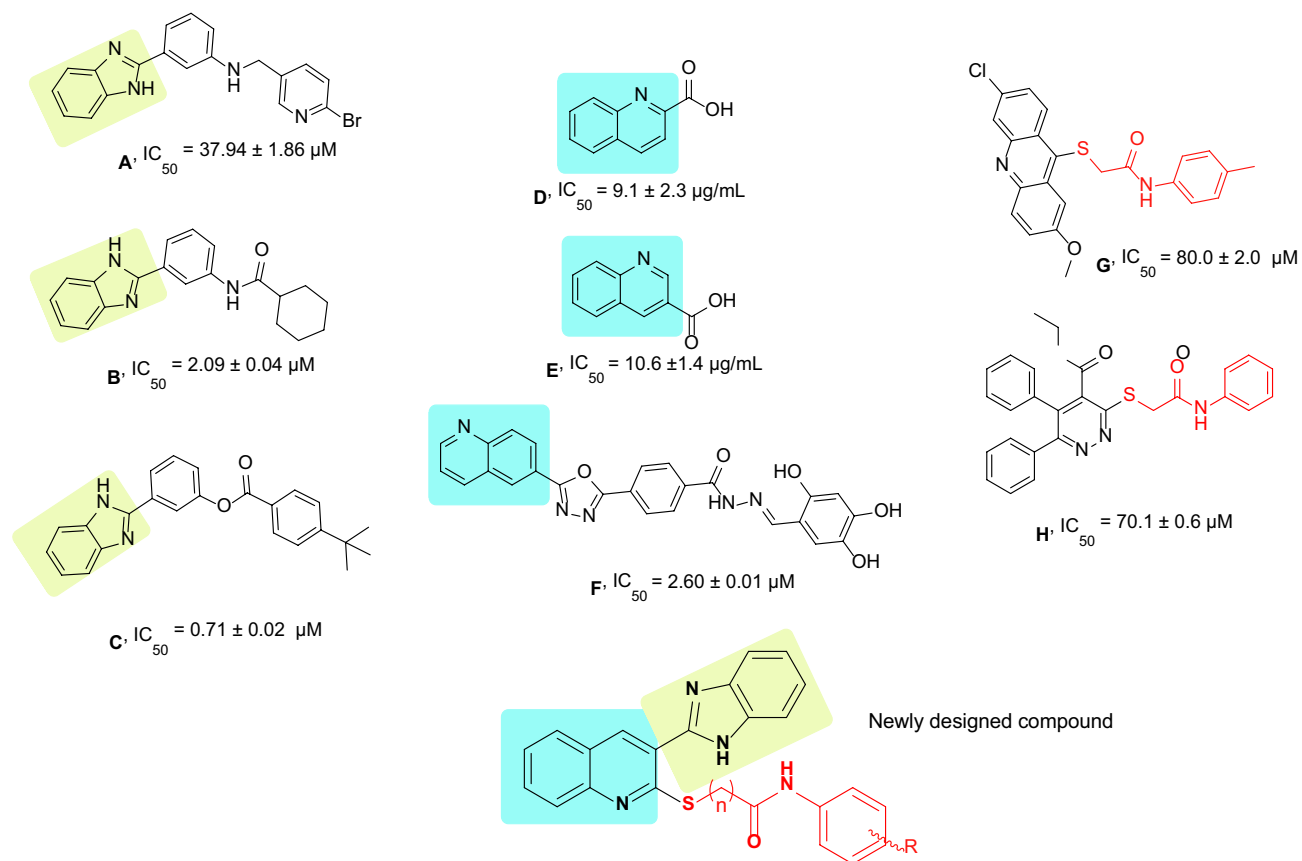


Figure 1. Schematic illustration of previously reported α -glucosidase inhibitors and newly designed compound.

Regarding promising anti-diabetic properties of quinolone heterocyclic scaffold and benzo[d]imidazole moiety, in this study, the novel series of quinoline-based-benzo[d]imidazole bearing different acetamide derivatives were synthesized, and evaluated for their inhibition potential against the α -glucosidase enzyme. Also, kinetic as well as molecular docking studies of the most potent compound were performed to evaluate their inhibition pattern against α -glucosidase.

Results and discussion

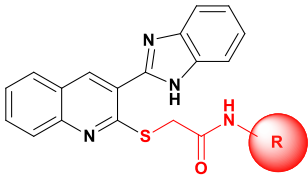
Design of quinoline-based-benzo[d]imidazole derivatives. During the last years, several non-sugar-based α -glucosidase inhibitors were identified. The random screening of the in-house library resulted in introducing compound **A** (Fig. 1) bearing benzo[d]imidazole moiety with good potency against α -glucosidase²⁰. The follow-up structural optimization of **A** resulted in a series of novel 2-phenyl-1H-benzo[d]imidazole derivatives (compound **B** and **C**) with IC_{50} values in the range of 0.71 to $> 100 \mu\text{M}$ compared to the acarbose as a positive control with an IC_{50} value of $258.53 \pm 1.27 \mu\text{M}$. Preliminary structure-activity relationships (SARs) study revealed that the benzo[d]imidazole core played key role in the inhibition of α -glucosidase activity¹⁷.

Also, recent studies demonstrated the α -glucosidase inhibitory activity of quinoline-containing compounds. The preliminary bioassay results revealed that compounds **D** and **E** (Fig. 1) had significant inhibitory potency compared to acarbose ($IC_{50} = 66.5 \pm 1.5 \mu\text{g/mL}$)²⁶. To further improve the α -glucosidase inhibitory activity of quinolone derivatives, the structural modification was carried out. These analogs exhibited inhibitory potential with IC_{50} values in the ranges between 2.60 and $102.12 \mu\text{M}$ (Compound **F**, Fig. 1)²⁷.

Furthermore, it was reported that methyl-thioacetamide moiety (compounds **G** and **H**) can not only improve α -glucosidase inhibition through generating optimum structure to effectively participate within the active site but also provide a suitable site for derivatization^{28–30}.

In this context, molecular hybridization as a powerful tool for drug designing was applied so that benzo[d]imidazole and quinoline as potent heterocyclic pharmacophores were conjugated to different acetamide derivatives. Novel designed compounds were synthesized and evaluated for their α -glucosidase inhibitory activities. Preliminary SAR studies were conducted. Further, kinetic study plus *in silico* assessments were performed to evaluate the binding of the active compound to the enzyme.

Chemistry. The synthesis of compounds **9a–r** is schematically shown in Fig. 2. Briefly, phosphoryl chloride in *N,N*-dimethylformamide (DMF) was added dropwise to the cold *N*-phenylacetamide (**1**) under reflux conditions for 15 h to obtain 2-chloroquinoline-3-carbaldehyde (**2**)³¹. Compound **2** and sodium sulfide were then dissolved in DMF and stirred at room temperature for 2 h to achieve 3-formyl-2-mercaptoquinoline (**3**)³². Then,



Compound	R	IC ₅₀ (μM) ^a	Concentrations of precipitation (μM)
9a	Phenyl	30.2 ± 0.4	≥ 200
9b	2-Fluorophenyl	61.3 ± 0.4	≥ 200
9c	4-Fluorophenyl	13.5 ± 0.6	≥ 200
9d	3-Chlorophenyl	3.2 ± 0.3	≥ 200
9e	4-Chlorophenyl	110.4 ± 0.2	≥ 200
9f	2-Bromophenyl	23.4 ± 0.2	≥ 200
9g	4-Bromophenyl	185.0 ± 0.3	≥ 200
9h	2,6-Dichlorophenyl	100.8 ± 0.1	≥ 200
9i	4-Nitrophenyl	19.7 ± 0.2	≥ 200
9j	2-Methylphenyl	16.5 ± 0.4	≥ 200
9k	4-Methylphenyl	12.3 ± 0.2	≥ 200
9l	4-Methoxyphenyl	5.7 ± 0.3	≥ 200
9m	4-Ethylphenyl	55.6 ± 0.2	≥ 200
9n	2,3-Dimethylphenyl	9.8 ± 0.5	≥ 200
9o	2,6-Dimethylphenyl	147.0 ± 0.2	≥ 200
9p	Naphthalene	17.7 ± 0.8	≥ 200
9q	Benzyl	750 <	≥ 200
9r	4-Fluorobenzyl	33.0 ± 0.1	≥ 200
Acarbose	–	750.0 ± 5.0	–

Table 1. α-Glucosidase inhibitory activity of compounds **9a–r**. ^aData represented in terms of mean ± SD.

disappointingly, **9o** bearing symmetric multi-substituted moiety (R = 2,6-diCH₃, IC₅₀ = 147.0 μM) recorded the reduction in the activity compared to **9n**. However, **9o** derivative still demonstrated around eightfold improvement in the potency compared to acarbose with IC₅₀ of 750.0 μM.

Precise assessments on the **9j–o** derivatives also indicated that the position of substitutions seems to have the most dominant role in the inhibition compared to the lipophilicity of moiety.

Ring substitution assessments were also performed in which phenyl (**9a**) was replaced with naphthyl (**9p**). An improvement in the activity showed that a bulk structure is more favorable.

Next, the investigation of SAR indicated that nitro (**9i**, IC₅₀ = 19.7 ± 0.2 μM) and methoxy (**9l**, IC₅₀ = 5.7 ± 0.3 μM) moieties were optimal substituents at the *para* position of phenylacetamide which improved the α-glucosidase inhibition. These results suggested that such substitution may probably enhance the ligand–protein interaction with the α-glucosidase active site.

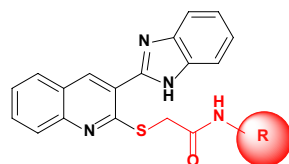
9q and **9r** were also synthesized to evaluate the role of elongation of the linker between aryl substitutions and thioacetamide moiety. Compound **9q** with benzyl substitution exhibited dramatic reduction in the α-glucosidase inhibition compared to **9a** which exhibited the destructive effect of elongation of the linker in the unsubstituted derivatives. Also, there was a similar trend in the potency in **9r** bearing 4-fluorobenzyl compared to **9c** (R = 4-Fluorophenyl).

The summary of the SARs to improve α-glucosidase inhibitory activity was depicted in Fig. 3. Overall, it can be understood that the most potent derivative (**9d**) exhibited better inhibitory activity against α-glucosidase compared to lead compounds including **A** to **G** reported in Fig. 1 concerning their positive control.

Enzyme kinetic studies. To gain insight into the mechanism of action of **9d** as the most potent α-glucosidase inhibitor, kinetic measurements were performed. According to Fig. 4a, the Lineweaver–Burk plot showed that the K_m gradually increased and V_{max} remained unchanged with increasing inhibitor concentration indicating a competitive inhibition. The results show **9d** bonded to the active site on the enzyme and compete with the substrate for binding to the active site. Furthermore, the plot of the K_m versus different concentrations of inhibitor gave an estimate of the inhibition constant, K_i of 3.2 μM (Fig. 4b).

Docking analyses. To identify the accuracy and validation of docking procedures, the self-docking of acarbose (as a crystallographic ligand) was performed through induced fit docking of Schrödinger software. Alignment of the best pose of acarbose in the active site of α-glucosidase and crystallographic ligand recorded an RMSD value of 1.73 Å (RMSD should be less than 2 Å) which confirms the accuracy of docking. Next, the same

Bulk EWG at *ortho* and *meta* position seems more favorable



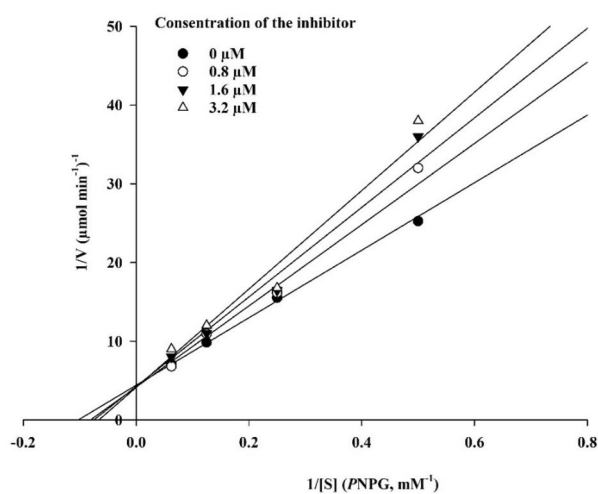
Spacious ring improve the activity

EDG showed overall improvement in the potency

Elongation of linker is not favorable

Figure 3. Summary of the SARs.

a)



b)

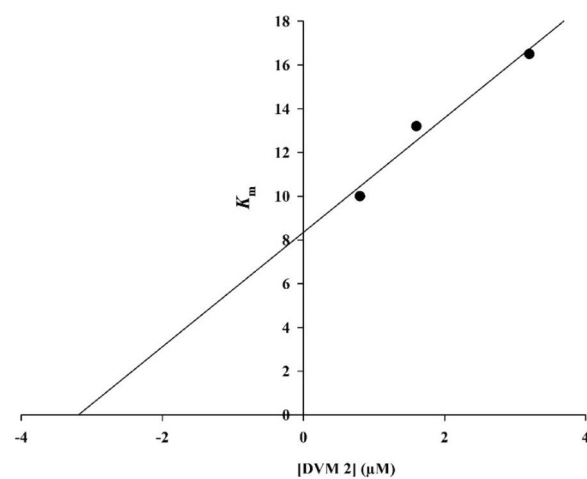


Figure 4. Kinetics of α -glucosidase inhibition by **9d**. (a) The Lineweaver–Burk plot in the absence and presence of different concentrations of **9d**; (b) the secondary plot between K_m and various concentrations of **9d**.

docking procedure was repeated with all derivatives and their binding to α -glucosidase was analyzed. Results are summarized in Table 2.

The in silico studies showed the binding energy of acarbose was -6.14 kcal/mol while the glide score value of **9a–r** ranges from -4.65 to -6.92 kcal/mol. As can be seen, the most potent derivative in in vitro assay was **9d** ($IC_{50} = 3.2 \pm 0.3$) > **9l** ($IC_{50} = 5.7 \pm 0.3 \mu\text{M}$) > **9n** ($IC_{50} = 9.8 \pm 0.5 \mu\text{M}$) > **9k** ($IC_{50} = 12.3 \pm 0.2 \mu\text{M}$) exhibited the best in silico results with glide score value of -6.92 , -6.33 , -6.90 and -6.72 kcal/mol, respectively. Assessments on least potent derivatives, **9q** ($IC_{50} > 750$), **9g** ($IC_{50} = 185.0 \pm 0.3$) and **9o** ($IC_{50} = 147.0 \pm 0.2$) reveal low binding interaction with the targeted enzyme with binding energy of -4.30 , -4.65 and -4.99 value.

The docking results between α -glucosidase and compound **9d** was shown in Fig. 5. Compound **9d** was well inserted into the active site and recorded a Glide score of -6.92 . Compound **9d** established critical hydrogen bond interaction with Trp481 and benzimidazole. Also, benzimidazole participated in π -cation interaction with Arg600. On the other side of the molecule, 3-chlorophenylacetamide established H-bond interaction with Asp616 and halogen-bound interaction with Leu677. Notably, in most derivatives, the designed scaffold participated in the critical interactions within the active site of the enzyme and showed similar kinds of interactions to the native ligand.

Conclusion

In this study, a series of novel quinoline-based-benzo[d]imidazole bearing different acetamide derivatives were designed, synthesized and their inhibitory activity against α -glucosidase was performed. Most of these derivatives showed increased activity compared to acarbose as the positive control. The analysis of the SAR indicated that *meta*-chlorine substitution, as well as polar group with potential hydrogen interactions at the R position, was beneficial to α -glucosidase inhibition. The most potent candidate in this series **9d** ($IC_{50} = 3.2 \pm 0.3 \mu\text{M}$) was chosen for further biological evaluation. The enzyme kinetics assessments indicated that compound **9d** inhibited α -glucosidase in a competitive inhibition manner ($K_i = 3.2 \mu\text{M}$). According to the docking study, compound **9d** was well fitted in the active site of α -glucosidase through both hydrophobic and hydrogen interactions. Overall, it can be understood that the most potent derivative (**9d**) exhibited better inhibitory activity against α -glucosidase compared to lead compounds including **A**, to **G** reported compared to positive control reported in Fig. 1. In silico assessments confirmed the critical role of benzimidazole and aryl-acetamides to participate in interactions with the binding site of an enzyme.

Regarding that T2DM is public health concern nowadays, the inhibition of α -glucosidase is considered an efficient approach to target T2DM. It was shown that quinoline-based-benzo[d]imidazole bearing different acetamides constructed a new nucleus which provided a significant role for α -glucosidase inhibition. However, to better extract the SARs of this set of compounds, in the future project, heteroaryl or aliphatic substituents at the R position will be synthesized. Also, bioisosteric replacement of benzo[d]imidazole with other heteroaromatic rings will increase our insight into the design of more potent α -glucosidase inhibitors.

Experimental

Chemistry. All the reagents were purchased from commercial sources. ^1H and ^{13}C NMR spectra were determined by a Bruker FT-400 MHz spectrometer in DMSO- d_6 . All the chemical shifts were reported as (δ) values ppm. The MS spectra were recorded using an Agilent 7890A spectrometer at 70 eV. CHNOS analysis was performed using ECS4010 Costech Company. IR spectra were obtained with a Nicolet, FR-IR Magna 550. Melting-point were also recorded using Kofler hot-stage apparatus.

Synthesis of 2-chloroquinoline-3-carbaldehyde (2)³¹. To N, N-dimethylformamide (70.0 mmol) in the round-bottomed flask, phosphorus oxychloride (120.0 mmol) was added dropwise and the reaction mixture was stirred for 1 h at 0 – 5 °C. To this flask, N-phenylacetamide (30.0 mmol) was added and stirred for an extra 30 min followed by refluxing for 5–4 h under N_2 atmosphere. After the reaction was completed (TLC monitoring), the mixture was poured into crushed ice under constant stirring. The precipitate obtained was vacuum filtered, washed with water, air-dried, and recrystallized from EtOAc to give the 2-chloroquinoline-3-carbaldehyde.

Synthesis of 2-mercaptoquinoline-3-carbaldehyde (3)³². The reaction was initiated by stirring the mixture of 2-chloroquinoline-3-carbaldehyde **2** (1 mmol) and sodium sulfide (1 mmol) for 2 h at room temperature in dry DMF (50 mL). Then, the reaction mixture was poured into crushed ice and made acidic with acetic acid. The product was filtered off, washed with water, and dried to give the desired 2-mercaptoquinoline-3-carbaldehyde that was further purified by recrystallization in ethanol.

Synthesis of 3-(1H-benzo[d]imidazol-2-yl)quinoline-2-thiol (5)³³. 2-Mercaptoquinoline-3-carbaldehyde (1 mmol) and o-phenylenediamine (1.2 mmol) were dissolved in 2 mL DMF. Under stirring at room temperature, 1 mmol of sodium metabisulfite is added and allowed to react at 120 °C for about 4 h. After completion of the reaction, the mixture was precipitated in ice water, filtered, and dried at room temperature.

Synthesis of 2-chloro-N-phenylacetamide derivatives (8a–r)³⁴. To a solution of aniline derivatives (1 mmol) in DMF (4 mL), chloroacetylchloride was added at 0 °C. The mixture was stirred at room temperature for 5 h and poured into water and then filtered to get the **8a–r**. The obtained solids were then filtered, dried, and recrystallized from ethanol.

Compound	R	Glide score	Amino acid	Type of interaction
9a	Phenyl	- 6.43	Asp616	H-bound
			Leu678	H-bound
			Phe649	Pi-pi stacking
9b	2-Fluorophenyl	- 5.81	Asp616	H-bound
			Asp282	H-bound
9c	4-Fluorophenyl	- 6.59	Trp376	Pi-pi stacking
			Trp481	Pi-pi stacking
			Leu677	H-bound
			Asp616	H-bound
			Arg600	Pi-cation
			Asp518	Salt bridge
9d	3-Chlorophenyl	- 6.92	Arg600	Pi-cation
			Trp481	H-bound
			Asp616	H-bound
			Asp616	H-bound
			Leu677	Halogen bound
9e	4-Chlorophenyl	- 5.39	Arg600	Pi-cation
			Asp282	H-bound
			Trp481	H-bound
9f	2-Bromophenyl	- 6.14	Arg600	Pi-cation
			Asp282	H-bound
			Trp481	H-bound
9g	4-Bromophenyl	- 4.65	Asp282	H-bound
			Trp481	Pi-pi stacking
			Phe649	Pi-pi stacking
9h	2,6-Dichlorophenyl	- 4.99	Trp481	Pi-pi stacking
			Trp481	Pi-pi stacking
			Trp481	Pi-pi stacking
			Phe649	Pi-pi stacking
			Phe649	Pi-pi stacking
9i	4-Nitrophenyl	- 6.31	Asp616	H-bound
			Asp282	H-bound
			Arg281	Pi-cation
9j	2-Methylphenyl	- 6.13	Asp616	H-bound
			Asp282	H-bound
			Phe525	Pi-pi stacking
9k	4-Methylphenyl	- 6.72	Phe649	Pi-pi stacking
			Phe649	Pi-pi stacking
			Asp616	H-bound
			Ser676	H-bound
9l	4-Methoxyphenyl	- 6.33	Leu677	H-bound
			Asp616	H-bound
			Phe649	Pi-pi stacking
			Trp481	Pi-pi stacking
9m	4-Ethylphenyl	- 6.54	Asp282	H-bound
			Asp282	H-bound
			Trp481	H-bound
9n	2,3-Dimethylphenyl	- 6.900	Asp616	H-bound
			Trp481	H-bound
			Phe649	Pi-pi stacking
9o	2,6-Dimethylphenyl	- 5.53	Asp616	H-bound
			Asp282	H-bound
Continued				

Compound	R	Glide score	Amino acid	Type of interaction
9p	Naphthalene	-6.25	Asp616	H-bound
			Asp616	H-bound
			Trp481	H-bound
			Phe525	Pi-pi stacking
			Trp376	Pi-pi stacking
9q	Benzyl	-4.30	Trp376	Pi-pi stacking
			Phe525	Pi-pi stacking
9r	4-Fluorobenzyl	-5.90	Asp282	H-bound
			Asp282	H-bound
			Trp376	Pi-pi stacking
			Trp481	Pi-pi stacking
			Trp481	Pi-pi stacking
Acarbose	-	-6.14	Asp616	H-bound
			Asp616	Salt bridge
			Asp518	H-bound
			Phe525	H-bound

Table 2. Docking scores and interactions of compounds against the α -glucosidase (PDB ID: 5NN8).

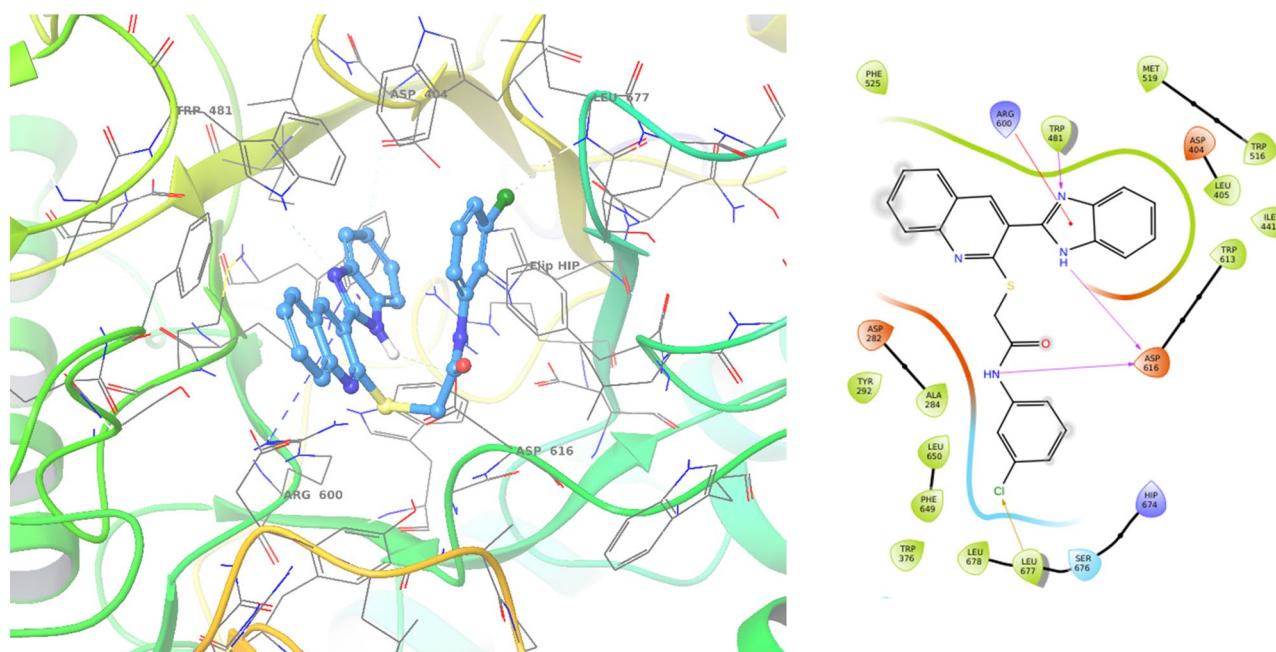


Figure 5. 3D and 2D proposed binding modes of compounds **9d** (blue color) with α -glucosidase.

General method for synthesis of 2-((3-(1H-benzo[d]imidazol-2-yl)quinolin-2-yl)thio)-N-phenylacetamide derivatives (9a-r)³⁵. A mixture of 3-(1H-benzo[d]imidazol-2-yl)quinoline-2-thiol (1 mmol) and potassium carbonate (1.5 mmol) in DMF were stirred at room temperature for 15–20 min. Afterward, N-chloroacetyl-aniline (1.2 mmol) was added to the above reaction mixture and stirred for an extra 4–5 h. After completion of the reaction, ice-cold water was added to the reaction mixture and stirred for 20 min. The obtained solid was filtered and washed with cold water several times. The acquired crude solid was purified by recrystallization from ethanol.

2-((3-(1H-benzo[d]imidazol-2-yl)quinolin-2-yl)thio)-N-phenylacetamide (9a). Brown solid; Yield: 93%; MP = 180–182 °C; IR (KBr, ν_{\max}) 3310 (NH), 3025 (C–H Aromatic), 2970 (CH₂ Aliphatic), 1675 (C=O) cm^{-1} ; ¹H NMR (400 MHz, DMSO-*d*₆) δ 10.71 (s, 1H, NH), 9.07 (s, 1H, H₃), 8.47 (s, 1H, H₄), 8.19 (d, *J* = 8.00 Hz, 1H, H₈), 8.10 (d, *J* = 8.60 Hz, 1H, H₅), 7.86 (t, *J* = 8.40 Hz, 1H, H₇), 7.81 (d, *J* = 7.6 Hz, 2H, H₂, H₆), 7.65 (t, *J* = 8.00 Hz, 1H, H₄), 7.41 (t, *J* = 7.90 Hz, 2H, H₃, H₅), 7.16 (t, *J* = 7.40 Hz, 1H, H₃) ppm. ¹³C NMR (100 MHz, DMSO-*d*₆): δ 167.80, 157.98, 148.94, 147.10, 143.98, 139.79, 136.69, 135.03, 131.63, 129.24, 128.79, 127.65, 126.76, 125.08,

123.74, 123.63, 123.20, 123.40, 119.78, 119.48, 112.01, 36.55 ppm; ESI-MS ($C_{24}H_{18}N_4OS$): calculated m/z 410.15 $[M+H]^+$, observed m/z 410.10 $[M+H]^+$ Anal. Calcd. For $C_{24}H_{18}N_4OS$ C, 70.22; H, 4.42; N, 13.65; Found: C, 70.39; H, 4.60; N, 13.76;

2-((3-(1H-benzo[d]imidazol-2-yl)quinolin-2-yl)thio)-N-(2-fluorophenyl)acetamide (9b). Brown solid; Yield: 87%; MP = 183–185 °C; IR (KBr, ν_{max}) 3325 (NH), 3060 (C–H Aromatic), 2950 (CH_2 Aliphatic), 1680 (C=O) Cm^{-1} ; 1H NMR (400 MHz, DMSO- d_6) δ 13.15 (s, 1H), 10.21 (s, 1H), 8.79 (s, 1H), 8.03 (d, $J=7.9$ Hz, 1H), 7.98 (d, $J=8.4$ Hz, 1H), 7.96–7.88 (m, 1H), 7.82 (t, $J=8.2$ Hz, 1H), 7.61 (t, $J=7.4$ Hz, 1H), 7.35–7.21 (m, 4H), 7.15–7.00 (m, 3H), 4.23 (s, 2H) ppm. ^{13}C NMR (100 MHz, DMSO- d_6): δ 168.45, 157.90, 154.95, 152.52 (CF, $^1J_{CF}=243$ Hz), 148.91, 147.12, 136.82, 131.63, 128.77, 127.64, 126.90, 126.84, 126.78, 125.48, 125.40, 125.14, 124.86, 124.04, 123.22, 116.00, 115.81, 35.95 ppm; ESI-MS ($C_{24}H_{17}FN_4OS$): calculated m/z 428.11 $[M+H]^+$, observed m/z 428.20 $[M+H]^+$, Anal. Calcd. for $C_{24}H_{17}FN_4OS$: C, 67.27; H, 4.00; N, 13.08; Found: C, 67.45; H, 4.18; N, 13.24;

2-((3-(1H-benzo[d]imidazol-2-yl)naphthalen-2-yl)thio)-N-(4-fluorophenyl)acetamide (9c). Brown solid; Yield: 89%; MP = 189–191 °C; IR (KBr, ν_{max}) 3330 (NH), 3025 (C–H Aromatic), 2915 (CH_2 Aliphatic), 1640 (C=O) Cm^{-1} ; 1H NMR (400 MHz, DMSO- d_6) δ 13.70 (s, 1H), 10.49 (s, 1H), 8.78 (s, 1H), 8.01 (d, $J=8.00$ Hz, 1H), 7.92 (d, $J=8.30$ Hz, 1H), 7.79 (t, $J=7.70$ Hz, 1H), 7.73–7.56 (m, 5H), 7.33–7.26 (m, 2H), 7.15 (t, $J=8.8$, 2H), 4.17 (s, 2H), ppm. ^{13}C NMR (100 MHz, DMSO- d_6): δ 159.57, 157.95 (CF, $^1J_{CF}=238.1$ Hz), 157.19, 148.96, 147.09, 136.68, 136.21, 131.63, 128.79, 127.3, 126.76, 125.08, 123.19, 121.25, 121.17, 115.92, 115.70, 36.49 ppm; ESI-MS ($C_{24}H_{17}FN_4OS$): calculated m/z 428.11 $[M+H]^+$, observed m/z 428.30 $[M+H]^+$, Anal. Calcd. for $C_{25}H_{18}FN_3OS$: C, 70.24; H, 4.24; N, 9.83; Found: C, 70.41; H, 4.47; N, 9.99.

2-((3-(1H-benzo[d]imidazol-2-yl)quinolin-2-yl)thio)-N-(3-chlorophenyl)acetamide (9d). Brown solid; Yield: 89%; MP = 190–192 °C; IR (KBr, ν_{max}) 3310 (NH), 3015 (C–H Aromatic), 2880 (CH_2 Aliphatic), 1645 (C=O) Cm^{-1} ; 1H NMR (400 MHz, DMSO- d_6) δ 13.6 (s, 1H), 10.65 (s, 1H), 8.79 (s, 1H), 8.01 (d, $J=8.10$ Hz, 1H), 7.93–7.77 (m, 4H), 7.66–7.50 (m, 3H), 7.10 (d, $J=8.00$ Hz, 1H), 4.18 (s, 3H) ppm. ^{13}C NMR (100 MHz, DMSO- d_6): δ 168.42, 167.60, 166.09, 162.75, 157.90, 150.04, 149.10, 147.06, 143.03, 141.29, 136.63, 136.21, 133.61, 131.56, 130.39, 128.76, 127.59, 126.73, 125.12, 123.23, 123.24, 123.02, 118.97, 117.86, 31.22 ppm; ESI-MS ($C_{24}H_{17}ClN_4OS$): calculated m/z 444.08, $[M+H]^+$, observed m/z 444.20, $[M+H]^+$; Anal. Calcd. $C_{24}H_{17}ClN_4OS$, C, 64.79; H, 3.85; N, 12.59; Found: C, 64.95; H, 4.02; N, 12.77.

2-((3-(1H-benzo[d]imidazol-2-yl)quinolin-2-yl)thio)-N-(4-chlorophenyl)acetamide (9e). Brown solid; Yield: 90%; MP = 185–187 °C IR (KBr, ν_{max}) 3275 (NH), 3030 (C–H Aromatic), 2980 (CH_2 Aliphatic), 1680 (C=O) Cm^{-1} ; 1H NMR (400 MHz, DMSO- d_6) δ 13.14 (s, 1H), 10.57 (s, 1H), 8.78 (s, 1H), 8.01 (d, $J=8.00$ Hz, 1H), 7.89 (d, $J=8.40$ Hz, 1H), 7.78 (t, $J=7.70$ Hz, 2H), 7.68 (d, $J=8.50$ Hz, 3H), 7.59 (t, $J=7.50$ Hz, 1H), 7.37 (d, $J=8.50$ Hz, 2H), 7.29 (d, $J=7.20$ Hz, 2H) ppm. ESI-MS ($C_{24}H_{17}ClN_4OS$): calculated m/z 444.08, $[M+H]^+$, observed m/z 444.20, $[M+H]^+$, ^{13}C NMR (100 MHz, DMSO- d_6): δ 168.06, 157.91, 148.93, 147.07, 138.77, 136.66, 131.64, 129.16, 128.79, 127.59, 127.14, 126.78, 125.05, 123.15, 120.99, 36.58 ppm; Anal. Calcd. for $C_{24}H_{17}ClN_4OS$, C, 64.79; H, 3.85; N, 12.59; Found: C, 64.95; H, 3.99; N, 12.79.

2-((3-(1H-benzo[d]imidazol-2-yl)quinolin-2-yl)thio)-N-(2-bromophenyl)acetamide (9f). Brown solid; Yield: 93%; MP = 181–183 °C; IR (KBr, ν_{max}) 3300 (NH), 3030 (C–H Aromatic), 2965 (CH_2 Aliphatic), 1655 (C=O) Cm^{-1} ; 1H NMR (400 MHz, DMSO- d_6) δ 13.14 (s, 1H), 10.43 (s, 1H), 8.77 (s, 1H), 8.01 (d, $J=7.90$ Hz, 1H), 7.93 (d, $J=8.40$ Hz, 1H), 7.80 (d, $J=5.50$ Hz, 1H), 7.78 (d, $J=6.1$ Hz, 1H), 7.67–7.56 (m, 3H), 7.35–7.24 (m, 4H), 7.04 (t, $J=7.3$ Hz, 1H) ppm. ESI-MS ($C_{24}H_{17}BrN_4OS$): calculated m/z 490.03, $[M+H]^+$, observed m/z 488.10, $[M+H]^+$, ^{13}C NMR (100 MHz, DMSO- d_6): δ 168.25, 157.53, 149.29, 147.09, 136.81, 136.69, 133.05, 131.53, 128.75, 128.52, 127.87, 126.91, 126.84, 125.93, 125.25, 123.60, 122.90, 116.69, 115.96, 35.84 ppm; Anal. Calcd. for $C_{24}H_{17}BrN_4OS$ C, 58.90; H, 3.50; N, 11.45; Found: C, 59.11; H, 3.69; N, 11.75.

2-((3-(1H-benzo[d]imidazol-2-yl)quinolin-2-yl)thio)-N-(4-bromophenyl)acetamide (9g). Brown solid; Yield: 95%; MP = 185–187 °C; IR (KBr, ν_{max}) 3340 (NH), 3025 (C–H Aromatic), 2870 (CH_2 Aliphatic), 1640 (C=O) Cm^{-1} ; 1H NMR (400 MHz, DMSO- d_6) δ 13.15 (s, 1H), 10.58 (s, 1H), 8.01 (d, $J=7.90$ Hz, 1H), 7.90 (d, $J=8.10$ Hz, 1H), 7.78 (t, $J=7.70$ Hz, 2H), 7.64 (d, $J=8.50$ Hz, 3H), 7.60–7.56 (m, 1H), 7.49 (d, $J=8.50$ Hz 2H), 7.35–7.25 (m, 2H), 4.17 (s, 2H) ppm. ESI-MS ($C_{24}H_{17}BrN_4OS$): calculated m/z 490.03, $[M+H]^+$, observed m/z 488.10, $[M+H]^+$, ^{13}C NMR (100 MHz, DMSO- d_6): δ 168.10, 157.91, 148.94, 147.08, 143.98, 139.19, 136.66, 135.04, 132.07, 131.63, 128.78, 127.60, 126.77, 125.08, 123.76, 123.16, 122.41, 121.49, 121.40, 119.78, 115.18, 112.02, 36.62 ppm; Anal. Calcd. for $C_{24}H_{17}BrN_4OS$; C, 58.90; H, 3.50; N, 11.45; Found: C, 59.05; H, 3.70; N, 11.62.

2-((3-(1H-benzo[d]imidazol-2-yl)quinolin-2-yl)thio)-N-(2,6-dichlorophenyl)acetamide (9h). Brown solid; Yield: 86%; MP = 188–190 °C; IR (KBr, ν_{max}) 3340 (NH), 3035 (C–H Aromatic), 2960 (CH_2 Aliphatic), 1675 (C=O) Cm^{-1} ; 1H NMR (400 MHz, DMSO- d_6) δ 13.15 (s, 1H), 9.92 (s, 1H), 8.81 (s, 1H), 8.03 (d, $J=8.00$ Hz, 1H), 7.97 (d, $J=8.40$ Hz, 1H), 7.86 (d, $J=8.80$ Hz, 1H), 7.81 (t, $J=7.30$ Hz, 1H), 7.75–7.57 (m, 4H), 7.37 (d, $J=8.80$ Hz, 1H), 7.33–7.25 (m, 2H) 4.26 (s, 2H) ppm. ESI-MS ($C_{24}H_{17}Cl_2N_4OS$): calculated m/z 478.10, $[M+H]^+$, observed m/z 444.20, $[M+H]^+$, ^{13}C NMR (100 MHz, DMSO- d_6): δ 168.85, 157.60, 148.88, 147.10, 136.88, 134.69, 131.65, 129.30, 129.25, 128.79, 128.08, 127.77, 126.91, 126.45, 126.23, 125.19, 123.24, 35.80 ppm; Anal. Calcd. for $C_{24}H_{16}Cl_2N_4OS$ C, 60.13; H, 3.36; N, 11.69; Found: C, 60.24; H, 3.49; N, 11.85.

2-((3-(1H-benzo[d]imidazol-2-yl)quinolin-2-yl)thio)-N-(4-nitrophenyl)acetamide (9j). Pale yellow solid; Yield: 93%; MP=180–182 °C; IR (KBr, ν_{\max}) 3320 (NH), 3020 (C–H Aromatic), 2965 (CH₂ Aliphatic), 1670 (C=O), 1555–1350 (NO₂) Cm⁻¹; ¹H NMR (400 MHz, DMSO-*d*₆) δ 13.60 (s, 1H), 11.80 (s, 1H), 8.79 (s, 1H), 8.24 (d, *J*=9.30 Hz, 1H), 8.01 (d, *J*=7.70 Hz, 1H), 7.91 (d, *J*=9.30, 2H), 7.86–7.74 (m, 3H), 7.63 (d, *J*=7.70 Hz, 1H), 7.57 (t, *J*=8.00 Hz, 1H), 7.35–7.25 (m, 2H), 4.21 (s, 2H) ppm. ESI–MS (C₂₄H₁₇N₅O₃S): calculated *m/z* 455.11, [M+H]⁺, observed *m/z* 455.20, [M+H]⁺, ¹³C NMR (100 MHz, DMSO-*d*₆): δ 169.12, 157.79, 148.91, 147.01, 145.99, 143.96, 142.54, 136.61, 135.04, 131.67, 128.80, 127.49, 126.81, 125.60, 125.08, 123.79, 123.04, 122.43, 119.79, 119.08, 112.02, 36.80 ppm; ESI–MS (C₂₄H₁₇N₅O₃S C): calculated *m/z* 455.11 [M+H]⁺, observed *m/z* 455.20 [M+H]⁺; Anal. Calcd. for C₂₄H₁₇N₅O₃S C, 63.29; H, 3.76; N, 15.38; Found: C, 63.49; H, 3.96; N, 15.55.

2-((3-(1H-benzo[d]imidazol-2-yl)naphthalen-2-yl)thio)-N-(*o*-tolyl)acetamide (9k). Brown solid; Yield: 86%; MP=179–181 °C; IR (KBr, ν_{\max}) 3360 (NH), 3070 (C–H Aromatic), 2980 (CH₂ Aliphatic), 1680 (C=O) Cm⁻¹; ¹H NMR (400 MHz, DMSO-*d*₆) δ 13.15 (s, 1H), 10.34 (s, 1H), 8.77 (s, 1H), 8.01 (d, *J*=6.60 Hz, 1H), 7.93 (d, *J*=7.10 Hz, 1H), 7.80 (d, *J*=7.40 Hz, 2H), 7.66–7.46 (m, 4H), 7.30 (t, *J*=9.50 Hz, 2H), 7.10 (d, *J*=8.10 Hz, 2H), 4.15 (s, 2H), 2.20 (s, 3H), ppm. ¹³C NMR (100 MHz, DMSO-*d*₆): δ 167.54, 158.01, 148.96, 147.11, 137.30, 136.70, 132.52, 131.61, 129.60, 128.77, 127.66, 126.74, 125.08, 123.23, 119.77, 119.51, 112.02, 36.54, 20.91 ppm; Anal. Calcd. for C₂₆H₂₁N₃OS: C, 73.73; H, 5.00; N, 9.92; Found: C, 73.92; H, 5.19; N, 10.11.

2-((3-(1H-benzo[d]imidazol-2-yl)naphthalen-2-yl)thio)-N-(*p*-tolyl)acetamide (9l). Cream solid; Yield: 91%; MP=181–183 °C; IR (KBr, ν_{\max}) 3345 (NH), 3040 (C–H Aromatic), 2900 (CH-Aliphatic), 1670 (C=O) Cm⁻¹; ¹H NMR (400 MHz, DMSO-*d*₆) δ 13.15 (s, 1H), 10.34 (s, 1H), 8.77 (s, 1H), 8.01 (d, *J*=7.30 Hz, 1H), 7.93 (d, *J*=7.70 Hz, 1H), 7.79 (t, *J*=7.70 Hz, 2H), 7.63–7.48 (m, 4H), 7.29 (s, 2H), 7.10 (d, *J*=8.20 Hz, 2H), 4.16 (s, 2H), 2.23 (s, 3H) ppm. ESI–MS (C₂₆H₂₁N₃OS): calculated *m/z* 424.14, [M+H]⁺, observed *m/z* 424.10, [M+H]⁺ ¹³C NMR (100 MHz, DMSO-*d*₆): δ 162.6, 160.2, 147.4, 141.2, 140.1, 136.5, 133.7, 132.2, 131.0, 129.4, 128.4, 128.3, 126.2, 126.0, 124.0, 120.9, 28.1, 16.1 ppm; Anal. Calcd. for C₂₆H₂₁N₃OS C, 73.73; H, 5.00; N, 9.92; Found: C, 73.82; H, 5.14; N, 9.99.

2-((3-(1H-benzo[d]imidazol-2-yl)quinolin-2-yl)thio)-N-(4-methoxyphenyl)acetamide (9m). Cream solid; Yield: 93%; MP=191–193 °C; IR (KBr, ν_{\max}) 3340 (NH), 3030 (C–H Aromatic), 2910 (CH-Aliphatic), 1680 (C=O) Cm⁻¹; ¹H NMR (400 MHz, DMSO-*d*₆) δ 13.14 (s, 1H), 10.27 (s, 1H), 8.77 (s, 1H), 8.02 (d, *J*=7.70 Hz, 1H), 7.95 (d, *J*=8.40 Hz, 1H), 7.80 (t, *J*=8.30 Hz, 1H), 7.59 (t, *J*=7.90 Hz, 1H), 7.54 (d, *J*=9.00 Hz, 2H), 7.34–7.25 (m, 2H), 6.88 (d, *J*=9.10 Hz, 1H), 4.15 (s, 2H), 3.71 (s, 3H) ppm. ¹³C NMR (100 MHz, DMSO-*d*₆): δ 167.23, 158.02, 155.60, 148.96, 147.12, 136.71, 132.94, 131.62, 128.78, 127.68, 126.75, 125.08, 123.24, 121.03, 114.33, 55.58, 36.43 ppm; ESI–MS (C₂₅H₂₀N₄O₂S): calculated *m/z* 424.14 [M+H]⁺, observed *m/z* 424.10 [M+H]⁺; Anal. Calcd. for C₂₅H₂₀N₄O₂S; C, 68.16; H, 4.58; N, 12.72; Found C, 68.35; H, 4.76; N, 12.90.

2-((3-(1H-benzo[d]imidazol-2-yl)quinolin-2-yl)thio)-N-(4-ethylphenyl)acetamide (9n). Brown solid; Yield: 93%; MP=178–180 °C; IR (KBr, ν_{\max}) 3300 (NH), 3020 (C–H Aromatic), 2975 (CH₂ Aliphatic), 1670 (C=O) Cm⁻¹; ¹H NMR (400 MHz, DMSO-*d*₆) δ 13.12 (s, 1H), 10.34 (s, 1H), 8.78 (s, 1H), 8.01 (d, *J*=8.00 Hz, 1H), 7.95 (d, *J*=8.40 Hz, 1H), 7.79 (t, *J*=7.30 Hz, 1H), 7.75–7.65 (m, 2H), 7.58 (t, *J*=7.60 Hz, 1H), 7.54 (d, *J*=8.40 Hz, 2H), 7.30 (d, *J*=6.10 Hz, 2H), 7.13 (d, *J*=8.30 Hz, 2H), 4.17 (s, 2H), 2.53 (d, *J*=7.70 Hz, 2H), 1.14 (t, *J*=7.30 Hz, 3H) ppm. ESI–MS (C₂₆H₂₂N₄OS): calculated *m/z* 438.55, [M+H]⁺, observed *m/z* 438.10, [M+H]⁺, ¹³C NMR (100 MHz, DMSO-*d*₆): δ 167.55, 158.00, 148.97, 147.11, 139.01, 137.47, 136.70, 131.61, 128.78, 128.41, 127.68, 126.75, 125.08, 123.24, 119.61, 36.52, 28.06, 16.18, 16.12 ppm; Anal. Calcd. for C₂₆H₂₂N₄OS; C, 71.21; H, 5.06; N, 12.78; Found: C, 71.39; H, 5.26; N, 12.97.

2-((3-(1H-benzo[d]imidazol-2-yl)quinolin-2-yl)thio)-N-(2,3-dimethylphenyl)acetamide (9o). Brown solid; Yield: 93%; MP=185–187 °C; IR (KBr, ν_{\max}) 3300 (NH), 3020 (C–H Aromatic), 2975 (CH₂ Aliphatic) 1675 (C=O) Cm⁻¹; ¹H NMR (400 MHz, DMSO-*d*₆) δ 13.6 (s, 1H), 9.76 (s, 1H), 8.79 (s, 1H), 8.03 (d, *J*=8.90 Hz, 1H), 8.01 (d, *J*=7.90 Hz, 1H), 7.83 (t, *J*=8.30 Hz, 1H), 7.61 (t, *J*=7.90 Hz, 1H), 7.30 (d, *J*=6.60, 2H), 7.15 (d, *J*=7.50 Hz, 1H), 7.06–6.92 (m, 4H), 4.22 (s, 1H), 2.20 (s, 3H), 2.02 (s, 3H), ppm. ¹³C NMR (100 MHz, DMSO-*d*₆): δ 167.73, 157.98, 149.00, 147.19, 137.38, 136.87, 136.66, 131.60, 131.57, 128.81, 127.77, 127.33, 126.77, 125.62, 125.15, 123.78, 123.39, 35.74, 20.59, 14.47 ppm; ESI–MS (C₂₆H₂₂N₄OS): calculated *m/z* 438.15 [M+H]⁺, observed *m/z* 438.10 [M+H]⁺; Anal. Calcd. for C₂₆H₂₂N₄OS C, 71.21; H, 5.06; N, 12.78; Found C, 71.39; H, 5.26; N, 12.91.

2-((3-(1H-benzo[d]imidazol-2-yl)quinolin-2-yl)thio)-N-(2,6-dimethylphenyl)acetamide (9p). Brown solid; Yield: 93%; MP=185–187 °C; IR (KBr, ν_{\max}) 3325 (NH), 3045 (C–H Aromatic), 2980 (CH₂ Aliphatic) 1665 (C=O) Cm⁻¹; ¹H NMR (400 MHz, DMSO-*d*₆) δ 13.11 (s, 1H), 9.57 (s, 1H), 8.77 (s, 1H), 8.03 (t, *J*=8.40 Hz, 2H), 7.84 (t, *J*=7.70 Hz, 1H), 7.62 (t, *J*=7.20 Hz, 2H), 7.35–7.25 (m, 2H), 7.07–6.98 (m, 4H), 4.24 (s, 1H), 2.05 (s, 6H) ppm. ESI–MS (C₂₆H₂₂N₄OS): calculated *m/z* 438.15 [M+H]⁺, observed *m/z* 438.10 [M+H]⁺, ¹³C NMR (100 MHz, DMSO-*d*₆): δ 162.6, 161.6, 147.4, 140.9, 139.5, 133.7, 132.7, 132.3, 131.0, 129.4, 128.9, 128.3, 127.9, 127.5, 126.3, 126.0, 123.3, 43.3 ppm; Anal. Calcd. for C₂₆H₂₂N₄OS C, 71.21; H, 5.06; N, 12.78; Found C, 71.39; H, 5.26; N, 12.91.

2-((3-(1H-benzo[d]imidazol-2-yl)quinolin-2-yl)thio)-N-(naphthalen-2-yl)acetamide (9q). Cream solid; Yield: 91%; MP=182–184 °C; IR (KBr, ν_{\max}) 3340 (NH), 3030 (C–H Aromatic), 2900 (CH-Aliphatic), 1670

(C=O) Cm^{-1} ; ^1H NMR (400 MHz, $\text{DMSO}-d_6$) δ 13.16 (s, 1H), 10.33 (s, 1H), 8.80 (s, 1H), 8.10 (d, $J=8.30$ Hz, 1H), 8.05 (d, $J=7.90$ Hz, 2H), 7.92 (d, $J=7.8$ Hz, 1H), 7.86–7.80 (m, 1H), 7.79–7.66 (m, 3H), 7.63 (d, $J=7.70$ Hz, 2H), 7.53–7.44 (m, 2H), 7.37 (t, $J=7.60$ Hz, 1H), 7.34–7.24 (m, 2H), 4.36 (s, 2H), ppm. ESI–MS ($\text{C}_{28}\text{H}_{20}\text{N}_4\text{O}_5$): calculated m/z 460.14 $[\text{M} + \text{H}]^+$, observed m/z 460.10 $[\text{M} + \text{H}]^+$; ^{13}C NMR (100 MHz, $\text{DMSO}-d_6$): δ 168.50, 149.01, 147.21, 136.87, 134.23, 134.13, 131.61, 128.84, 128.54, 128.40, 127.79, 126.80, 126.46, 126.10, 126.06, 125.83, 125.18, 123.40, 122.18, 35.94 ppm; Anal. Calcd. for $\text{C}_{28}\text{H}_{20}\text{N}_4\text{O}_5$; C, 73.02; H, 4.38; N, 12.17; Found: C, 73.32; H, 4.55; N, 12.34.

2-((3-(1H-benzo[d]imidazol-2-yl)quinolin-2-yl)thio)-N-benzylacetamide (9r). Brown solid; Yield: 94%; MP = 183–185 °C; IR (KBr, ν_{max}) 3310(NH), 3045(C–H Aromatic), 2975 (CH_2 Aliphatic) 1655 (C=O) Cm^{-1} ; ^1H NMR (400 MHz, $\text{DMSO}-d_6$) δ 13.11 (s, 1H), 8.76 (s, 1H), 8.71 (t, $J=6.00$ Hz, 1H), 8.03 (d, $J=8.00$ Hz, 1H), 7.90 (d, $J=8.5$ Hz, 1H), 7.81 (t, $J=7.70$ Hz 1H), 7.62 (t, $J=7.60$ Hz, 2H), 7.34–7.25 (m, 2H), 7.21–7.13 (m, 6H), 4.31 (d, $J=6.00$ Hz, 2H), 4.06 (s, 1H) ppm. ESI–MS ($\text{C}_{26}\text{H}_{22}\text{N}_4\text{O}_5$): calculated m/z 424.14 $[\text{M} + \text{H}]^+$, observed m/z 424.10 $[\text{M} + \text{H}]^+$; ^{13}C NMR (100 MHz, $\text{DMSO}-d_6$): δ 168.67, 157.83, 149.00, 147.15, 139.83, 136.79, 131.51, 128.73, 128.55, 127.90, 127.45, 127.05, 126.73, 125.10, 123.39, 42.83, 35.17 ppm; Anal. Calcd. for $\text{C}_{25}\text{H}_{20}\text{N}_4\text{O}_5$: C, 70.73; H, 4.75; N, 13.20; Found: C, 70.92; H, 4.90; N, 13.38.

2-((3-(1H-benzo[d]imidazol-2-yl)quinolin-2-yl)thio)-N-(4-fluorobenzyl)acetamide (9s). Brown solid; Yield: 89%; MP = 186–188 °C; IR (KBr, ν_{max}) 3350 (NH), 3060 (C–H Aromatic), 2975 (CH_2 Aliphatic), 1670 (C=O) cm^{-1} ; ^1H NMR (400 MHz, $\text{DMSO}-d_6$) δ 8.74 (d, $J=14.20$ Hz, 2H), 8.01 (d, $J=8.00$ Hz, 1H), 7.90–7.75 (m, 2H), 7.70 (s, 2H), 7.60 (s, 1H), 7.39–7.17 (m, 4H), 6.95 (t, $J=8.9$, 2H), 4.29 (s, 2H), 4.04 (s, 2H), ppm. ESI–MS ($\text{C}_{25}\text{H}_{19}\text{FN}_4\text{O}_5$): calculated m/z 442.14 $[\text{M} + \text{H}]^+$, observed m/z 442.10 $[\text{M} + \text{H}]^+$; ^{13}C NMR (100 MHz, $\text{DMSO}-d_6$): δ 168.75, 162.67, 160.27 (CF, $^1J_{\text{CF}}=248.00$ Hz), 157.81, 149.10, 147.10, 136.74, 136.04, 131.43, 129.49, 129.41, 128.71, 127.84, 126.71, 125.10, 123.45, 122.98, 115.30, 115.10, 42.20, 35.21 ppm; Anal. Calcd. for $\text{C}_{25}\text{H}_{19}\text{FN}_4\text{O}_5$: C, 67.86; H, 4.33; N, 12.66; Found: C, 68.04; H, 4.52; N, 12.81.

α -Glucosidase inhibitory assay. The α -glucosidase inhibitory activities of all synthesized derivatives were assayed according to the previously reported procedure^{9,36}.

Enzyme kinetic studies. The mode of inhibition of the most active compound (9c), identified with the lowest IC_{50} , was investigated against α -glucosidase at different concentrations of *p*-nitrophenyl α -D-glucopyranoside (4–16 mM) as substrate in the absence and presence of 9c at different concentrations (0, 0.8, 1.6, and 3.2 μM). A Lineweaver–Burk plot was generated to identify the type of inhibition and the Michaelis–Menten constant (K_m) value was determined from the plot between reciprocal of the substrate concentration ($1/[\text{S}]$) and reciprocal of enzyme rate ($1/V$) over various inhibitor concentrations. The experimental inhibitor constant (K_i) value was constructed by secondary plots of the inhibitor concentration $[\text{I}]$ versus K_m ⁶.

Molecular docking. To perform the molecular modeling investigations, the Maestro Molecular Modeling platform (version 10.5) by Schrödinger, LLC was used. The X-ray crystal structure of the receptor was downloaded from the PDB database (PDB ID: 5NN8). The protein is then prepared using a protein preparation wizard. At this point, all water molecules and co-crystallized ligands were removed, the missing side chains and loops were filled using the prime tool, and PROPKA assigned H-bonds at pH 7.4. To prepare the ligands, the 2D structures of the ligands were drawn in ChemDraw (ver. 16) and converted into SDF files, which were used further by the ligprep module. Ligands were prepared by OPLS_2005 force field using EPIK at a target pH of 7.0 ± 2 . The grid box was generated for each binding site using entries with a box size of 25 Å, all derivatives were docked on binding sites using induced-fit docking, reporting 10 poses per ligand to form the final complex^{9,37}.

Data availability

All data generated or analyzed during this study are included in this published article and its Supplementary Information files.

Received: 7 February 2022; Accepted: 11 August 2022

Published online: 18 August 2022

References

- Roglic, G. WHO Global report on diabetes: A summary. *Int. J. Noncommun. Dis.* **1**(1), 3 (2016).
- Kondo, H., Taguchi, M., Inoue, Y., Sakamoto, F. & Tsukamoto, G. Synthesis and antibacterial activity of thiazolo-, oxazolo-, and imidazolo [3, 2-a][1, 8] naphthyridinecarboxylic acids. *J. Med. Chem.* **33**(7), 2012–2015 (1990).
- Adeghate, E., Schattner, P. & Dunn, E. An update on the etiology and epidemiology of diabetes mellitus. *Ann. N. Y. Acad. Sci.* **1084**(1), 1–29 (2006).
- Mora-Fernández, C. *et al.* Diabetic kidney disease: From physiology to therapeutics. *J. Physiol.* **592**(18), 3997–4012 (2014).
- Guariguata, L. *et al.* Global estimates of diabetes prevalence for 2013 and projections for 2035. *Diabetes Res. Clin. Pract.* **103**(2), 137–149 (2014).
- Karami, M. *et al.* One-pot multi-component synthesis of novel chromeno[4,3-b]pyrrol-3-yl derivatives as alpha-glucosidase inhibitors. *Mol. Divers.* <https://doi.org/10.1007/s11030-021-10337-w> (2021).
- Sohrabi, M. *et al.* A review on α -glucosidase inhibitory activity of first row transition metal complexes: A futuristic strategy for treatment of type 2 diabetes. *RSC Adv.* **12**(19), 12011–12052 (2022).
- Seltzer, H. S., Allen, E. W., Herron, A. L. & Brennan, M. T. Insulin secretion in response to glycemic stimulus: Relation of delayed initial release to carbohydrate intolerance in mild diabetes mellitus. *J. Clin. Investig.* **46**(3), 323–335 (1967).

9. Moghaddam, F. M. *et al.* Synthesis and characterization of 1-amidino-O-alkylureas metal complexes as α -glucosidase Inhibitors: Structure-activity relationship, molecular docking, and kinetic studies. *J. Mol. Struct.* **1250**, 131726 (2022).
10. Iraj, A. *et al.* Cyanoacetohydrazide linked to 1, 2, 3-triazole derivatives: A new class of α -glucosidase inhibitors. *Sci. Rep.* **12**(1), 1–15 (2022).
11. Tundis, R., Loizzo, M. & Menichini, F. Natural products as α -amylase and α -glucosidase inhibitors and their hypoglycaemic potential in the treatment of diabetes: An update. *Mini Rev. Med. Chem.* **10**(4), 315–331 (2010).
12. Pedrood, K. *et al.* Design, synthesis, characterization, enzymatic inhibition evaluations, and docking study of novel quinazolinone derivatives. *Int. J. Biol. Macromol.* **170**, 1–12 (2021).
13. Gulçin, İ *et al.* Antidiabetic and antiparasitic potentials: Inhibition effects of some natural antioxidant compounds on α -glucosidase, α -amylase and human glutathione S-transferase enzymes. *Int. J. Biol. Macromol.* **119**, 741–746 (2018).
14. Kumar, S., Narwal, S., Kumar, V. & Prakash, O. α -Glucosidase inhibitors from plants: A natural approach to treat diabetes. *Pharmacogn. Rev.* **5**(9), 19 (2011).
15. Abbas, G., Al Harrasi, A., Hussain, H., Hamaed, A. & Supuran, C. T. The management of diabetes mellitus-imperative role of natural products against dipeptidyl peptidase-4, α -glucosidase and sodium-dependent glucose co-transporter 2 (SGLT2). *Bioorg. Chem.* **86**, 305–315 (2019).
16. Wali, S. *et al.* Synthesis of new clioquinol derivatives as potent α -glucosidase inhibitors; molecular docking, kinetic and structure-activity relationship studies. *Bioorg. Chem.* **119**, 105506 (2021).
17. Dhameja, M. & Gupta, P. Synthetic heterocyclic candidates as promising α -glucosidase inhibitors: An overview. *Eur. J. Med. Chem.* **176**, 343–377 (2019).
18. Nasli Esfahani, A. *et al.* Design and synthesis of phenoxymethylbenzoimidazole incorporating different aryl thiazole-triazole acetamide derivatives as α -glucosidase inhibitors. *Mol. Divers.* **26**, 1995 (2021).
19. Zarenezhad, E., Montazer, M. N., Tabatabaee, M., Irajie, C. & Iraj, A. New solid phase methodology for the synthesis of biscoumarin derivatives: Experimental and in silico approaches. *BMC Chem.* **16**(1), 53 (2022).
20. Li, Y. *et al.* Discovery of new 2-phenyl-1H-benzo[d]imidazole core-based potent α -glucosidase inhibitors: Synthesis, kinetic study, molecular docking, and in vivo anti-hyperglycemic evaluation. *Bioorg. Chem.* **117**, 105423 (2021).
21. Abbasi, I. *et al.* Isatin-hydrazide conjugates as potent α -amylase and α -glucosidase inhibitors: Synthesis, structure and invitro evaluations. *Bioorg. Chem.* **116**, 105385 (2021).
22. Xie, H.-X. *et al.* Novel tetrahydrobenzo[b]thiophen-2-yl)urea derivatives as novel α -glucosidase inhibitors: Synthesis, kinetics study, molecular docking, and in vivo anti-hyperglycemic evaluation. *Bioorg. Chem.* **115**, 105236 (2021).
23. Zarenezhad, E., Farjam, M. & Iraj, A. Synthesis and biological activity of pyrimidines-containing hybrids: Focusing on pharmacological application. *J. Mol. Struct.* **1230**, 129833 (2021).
24. Santos, C. M. M., Freitas, M. & Fernandes, E. A comprehensive review on xanthone derivatives as α -glucosidase inhibitors. *Eur. J. Med. Chem.* **157**, 1460–1479 (2018).
25. Sari, S., Barut, B., Özel, A. & Saraç, S. Discovery of potent α -glucosidase inhibitors through structure-based virtual screening of an in-house azole collection. *Chem. Biol. Drug Des.* **97**, 701 (2020).
26. Lee, H.-W., Yang, J.-Y. & Lee, H.-S. Quinoline-2-carboxylic acid isolated from *Ephedra pachyclada* and its structural derivatives show inhibitory effects against α -glucosidase and α -amylase. *J. Korean Soc. Appl. Biol. Chem.* **57**(4), 441–444 (2014).
27. Taha, M. *et al.* Novel quinoline derivatives as potent in vitro α -glucosidase inhibitors: In silico studies and SAR predictions. *Med-ChemComm.* **6**(10), 1826–1836 (2015).
28. Mohammadi-Khanapostani, M. *et al.* Design, synthesis, docking study, α -glucosidase inhibition, and cytotoxic activities of acridine linked to thioacetamides as novel agents in treatment of type 2 diabetes. *Bioorg. Chem.* **80**, 288–295 (2018).
29. Ansari, S. *et al.* Design, synthesis, and α -glucosidase-inhibitory activity of phenoxy-biscoumarin-N-phenylacetamide hybrids. *Archiv. der Pharm.* **354**, e2100179 (2021).
30. Moghimi, S. *et al.* Design and synthesis of novel pyridazine N-aryl acetamides: In-vitro evaluation of α -glucosidase inhibition, docking, and kinetic studies. *Bioorg. Chem.* **102**, 104071 (2020).
31. Suman, P., Patel, B. P., Kasibotla, A. V., Solano, L. N. & Jonnalagadda, S. C. Synthesis and evaluation of functionalized aminobenzoboroxoles as potential anti-cancer agents. *J. Organomet. Chem.* **798**, 125–131 (2015).
32. Shashikumar, N. D., Krishnamurthy, G., Bhojyanaik, H. S., Lokesh, M. R. & Jithendrakumara, K. S. Synthesis of new biphenyl-substituted quinoline derivatives, preliminary screening and docking studies. *J. Chem. Sci.* **126**(1), 205–212 (2014).
33. Celik, I., Ayhan-Kilcigil, G., Karayel, A., Guven, B. & Onay-Besikci, A. Synthesis, molecular docking, in silico ADME, and EGFR kinase inhibitor activity studies of some new benzimidazole derivatives bearing thiosemicarbazide, triazole, and thiadiazole. *J. Heterocycl. Chem.* **59**(2), 371–387 (2022).
34. Flipo, M. *et al.* Discovery of novel N-phenylphenoxyacetamide derivatives as EthR inhibitors and ethionamide boosters by combining high-throughput screening and synthesis. *J. Med. Chem.* **55**(14), 6391–6402 (2012).
35. Kiran, B. M., Nandeshwarappa, B. P., Vaidya, V. P. & Mahadevan, K. M. Chemistry of substituted quinolines: Thieno [2, 3-b] and thiopyrano [2, 3-b] quinolines. *Phosphorus Sulfur Silicon Relat. Elem.* **182**(5), 969–980 (2007).
36. Shareghi-Boroujeni, D. *et al.* Synthesis, in vitro evaluation, and molecular docking studies of novel hydrazineylideneindolinone linked to phenoxymethyl-1, 2, 3-triazole derivatives as potential α -glucosidase inhibitors. *Bioorg. Chem.* **111**, 104869 (2021).
37. Iraj, A. *et al.* Cyanoacetohydrazide linked to 1, 2, 3-triazole derivatives: A new class of α -glucosidase inhibitors. *Sci. Rep.* **12**(1), 8647 (2022).

Author contributions

M.N. synthesized compounds. A.D. synthesized compounds. A.I. performed docking study and contributed to the preparation of the manuscript. M.A. performed chemical analysis. N.D. and M.A. contributed to the design and characterization of compounds. M.K. performed the biological assay. M.M.K. synthesized compounds. S.M. contributed to the design and characterization of compounds. M.D. supervised the biological tests. M.A.F. supervised the biological tests. B.L. contributed to the design and characterization of compounds. M.A. supervised all phases of the study. M.M. supervised all phases of the study. All authors reviewed the manuscript.

Funding

The authors wish to thank the financial support of National Institute for Medical Research Development (NIMAD) (Grant Number: 4000379) and the Research Council of Tehran University of Medical Sciences and Health Services (Grant Number: 1400-2-411-53423), Tehran, Iran.

Competing interests

The authors declare no competing interests.

Additional information

Supplementary Information The online version contains supplementary material available at <https://doi.org/10.1038/s41598-022-18455-7>.

Correspondence and requests for materials should be addressed to M.A. or M.M.

Reprints and permissions information is available at www.nature.com/reprints.

Publisher's note Springer Nature remains neutral with regard to jurisdictional claims in published maps and institutional affiliations.



Open Access This article is licensed under a Creative Commons Attribution 4.0 International License, which permits use, sharing, adaptation, distribution and reproduction in any medium or format, as long as you give appropriate credit to the original author(s) and the source, provide a link to the Creative Commons licence, and indicate if changes were made. The images or other third party material in this article are included in the article's Creative Commons licence, unless indicated otherwise in a credit line to the material. If material is not included in the article's Creative Commons licence and your intended use is not permitted by statutory regulation or exceeds the permitted use, you will need to obtain permission directly from the copyright holder. To view a copy of this licence, visit <http://creativecommons.org/licenses/by/4.0/>.

© The Author(s) 2022